Molecular Dynamics Simulation of Taylor-Couette Vortex Formation

D. Hirshfeld and D. C. Rapaport
Physics Department, Bar-Ilan University, Ramat-Gan 52900, Israel
(Received 31 December 1997)

The formation of toroidal Taylor vortices in a fluid contained within the annular region bounded by two concentric cylinders, the inner one of which rotates, has been observed using molecular dynamics simulation. The quantitative nature of the vortices has been examined over a range of supercritical Taylor numbers. The Fourier amplitudes of the fundamental radial velocity mode and its low-order harmonics have been analyzed; despite the microscopic system size their functional dependence on the Taylor number is in excellent agreement with theory and experiment. [S0031-9007(98)06397-2]

PACS numbers: 47.32.Cc, 02.70.Ns, 47.15.–x, 47.20.–k

One of the many fascinating instabilities that occur in hydrodynamics is the formation of toroidal vortices in a fluid confined to an annular gap between concentric rotating cylinders. The phenomenon is named after Taylor, who carried out experimental studies and provided a hydrodynamic stability analysis of the effect [1]. In this Letter we report on a numerical study of this flow instability at the atomistic level using a molecular dynamics approach. The simulations will be shown to not only produce the same kind of flow patterns as are observed experimentally, but to do this in a quantitatively correct manner.

Consider an experimental cell for which the inner and outer cylinder radii are r_i and r_o, with $d = r_o - r_i$ the width of the annulus, and $\eta = r_i/r_o$ the radius ratio. If the outer cylinder is at rest, and the angular velocity of the inner cylinder is ω, then the nature of the flow depends on the dimensionless Taylor number, $T = 4[(1 - \eta)/(1 + \eta)]R^2$, where $R = r_i d\omega/\nu$ is the Reynolds number, and ν the kinematic viscosity [2] (the more general case where the outer cylinder also rotates is not considered here). At low T the flow is purely azimuthal (Couette flow), but at a critical value, T_c, secondary flow patterns appear that have the form of regularly spaced axisymmetric vortices. A perturbation treatment of the Navier-Stokes equations [3] provides the basis for computing T_c in terms of the flow parameters. At higher T additional laminar instabilities appear (azimuthal waves), and eventually turbulence [4].

Various experimental techniques have been used to measure one or more components of the flow velocity field, which can be analyzed to establish the dependence on $\epsilon = (T - T_c)/T_c$ (or the corresponding quantity based on R). These techniques include ion conduction [5], anemometry [6], and laser-Doppler velocity probes [7–10]; between them, the experiments have examined all three velocity components (radial, azimuthal, and axial). The spatially varying velocity fields can be Fourier analyzed; this allows the determination of the ϵ dependence of both the fundamental mode that dominates the vortex structure, and the leading-order harmonics that account for deviations from a purely sinusoidal form. The behavior has been shown to agree with the predictions of a theoretical analysis of the Taylor instability [11], namely, that the coefficients A_n in the Fourier expansion for (e.g.) the radial velocity at a fixed radial distances from the axis, as a function of axial position z,

$$v_r(z, \epsilon) = \sum_{n \geq 1} A_n(\epsilon) \cos(nq[z + z_0]), \qquad (1)$$

where q is the wave number of the fundamental mode, can be expanded as

$$A_n(\epsilon) = a_n \epsilon^{n/2}(1 + a_{n1}\epsilon + a_{n2}\epsilon^2 + \ldots). \qquad (2)$$

The offset z_0 is included to allow a limited amount of variation in the axial positions of the vortices. While ϵ is ostensibly a small quantity, the results are found to obey these predictions over a much larger range. (The problem has also been studied by means of computational fluid dynamics [12].)

Molecular dynamics (MD) methods have, over the past decade, been used in the study of flow instability at microscopic scales. Work has been confined to two-dimensional flows: both vortex shedding in obstructed flow [13] and convective roll formation in the Rayleigh-Bénard problem [14] have been modeled. The surprising outcome of these simulations is not only that familiar macroscopic phenomena are reproduced in such minuscule systems—the typical size is no more than a few hundred angstroms—but that quantitative aspects of the behavior also agree with continuum results. The obvious question of whether the kinds of systems that can be handled by MD simulation in three dimensions are adequate to reproduce structured flow behavior typified by the Taylor instability has not been addressed to date. As will become eminently clear from this first application of MD to complex three-dimensional flows, not only does MD reproduce the phenomenon, it does so in excellent quantitative agreement with theory and experiment, microscopic system size (and other deviations from macroscopic fluid behavior) notwithstanding.

We consider a soft-sphere fluid in which particles interact through a short-range repulsive potential, $V(r) = 4\epsilon[(\sigma/r)^{12} - (\sigma/r)^6]$, with a cutoff at $r_c = 2^{1/6}\sigma$. Reduced MD units are employed in which $\sigma = 1$ and $\epsilon = 1$.

Standard MD techniques [15], with certain additional features that are described below, are used in carrying out the simulations; the equations of motion are integrated using the leapfrog method, with a time step of 0.005 (MD units).

The curved cylinder walls act as both nonslip boundaries and thermal reservoirs. The walls themselves are geometrically smooth. In order to produce a nonslip effect, each particle colliding with the wall has all memory of its previous velocity erased, and is reflected back into the system with a new velocity having a random direction and fixed magnitude; for the wall corresponding to the rotating inner cylinder the local (tangential) wall velocity is added to this vector. This mechanism is sufficient to drive the fluid rotation and dissipate the thermal energy generated by the sheared flow. The top and bottom end caps of the annular region are stationary and reflect incident particles elastically; the use of slip boundaries at the ends avoids creating a second source of sheared flow that would distort the vortices (an effect that is unavoidable experimentally).

In order to reduce the number of particles required for the simulation only one quadrant of the annular cell is explicitly modeled. Special periodic boundaries are used to account for the effect of particles in the absent quadrants: whenever a particle exits through either of these boundaries it is returned via the perpendicular boundary with position and velocity components suitably interchanged and sign-adjusted; interactions across these boundaries are also treated appropriately. Provided the secondary flows are axisymmetric this modification should not alter the behavior; experiment [16] indicates that if η is not too small, effects such as wavy vortices appear only for $R \gg R_c$ and, furthermore, this class of instability is suppressed unless $L \gg d$ [17].

The results described here are for cylinders with radii $r_i = 50$ and $r_o = 75$ ($\eta = 2/3$), and a series of angular velocities in the range $\omega = 0.05$–0.1. Each simulation run begins with the particles situated on the sites of a lattice between the two cylinders and assigned random initial velocities. The inner cylinder is initially at rest, but is gradually accelerated to the correct ω over the first 10^5 steps of the run.

The annular width ($d = 25$) is practically the smallest for which well-developed vortices can be readily observed; a width of only 20 leads to the much slower development of unstable vortices. Given that experimentally observed vortices have an almost square cross section (a result also predicted by theory), the system length is set to $L = 100$; consequently, if vortex formation actually occurs, four vortices should develop. This indeed is exactly what happens. Preliminary examination of other cylinder lengths shows that for $L = 75$ there are also four rolls, but only two at $L = 50$, whereas for $L = 125$ six rolls manage to form. Roll nucleation occurs near the end caps; the number of rolls is always even, and at the cylinder ends the radial flow is directed inwards.

Despite the limited system size and the use of only one quadrant these simulations nevertheless require 125 000 particles in order to ensure a mean density $\rho \approx 0.5$. Examination of the time dependence of the flow components reveals that while the final azimuthal velocity is reached after approximately 10^5 steps, the radial velocity (an estimate based on the average of the maximum absolute inward and outward values) requires twice as long to achieve its final state for the largest ω considered, and six times as long for the smallest. Measurements were begun only after the system had reached a steady flow state.

Because of the comparatively large systems and the long sequences of time steps required, the computations were carried out on a parallel computer. Four processing nodes of an IBM/SP2 were used; the system was subdivided into slabs along the cylinder axis and the contents of the slabs assigned to distinct nodes. Each slab can be processed almost independently, except for particles near slab boundaries whose coordinates must be shared between the nodes responsible for the adjacent slabs, and the possible movement of particles between slabs [15].

The time-dependent evolution of the flow observed for $\omega = 0.1$ (the highest rotation rate considered) is summarized in Fig. 1 as a sequence of snapshots showing streamlines derived from the radial and axial velocity components of the azimuthally averaged flow. A selection of images corresponding to key stages of the run is shown (t denotes the time); each image represents the average over 5000 steps using a 25×100 spatial grid for averaging the particle velocities in the radial and axial directions. The final state shown—a set of four counterrotating (toroidal) Taylor vortices—persists for the remainder of the run ($\approx 10^6$ steps).

The radial increase in the axially averaged density is found to be almost linear, and at $\omega = 0.1$ the total variation across the annulus is $\approx 25\%$; for smaller ω the density variation is reduced. There is also a smaller axial density variation that is almost sinusoidal. While it is clear that this system is not the incompressible fluid addressed by hydrodynamics, the deviations are by no means excessive. It turns out that only a limited range of ρ values is useful: lower ρ implies fewer particles, but at the same time the systematic density variations across the system become larger, which in turn makes comparison with theory questionable; at higher ρ, vortex formation becomes more difficult. The choice of ρ for this work therefore represents a compromise.

The axial dependence of the mean (azimuthally and radially averaged) radial velocity, $v_r(z)$, is shown in Fig. 2 for several ω values. The results are based on 20 sets of measurements over the final 10^5 steps, and their rms spread provides the error estimates. Both these results, and the corresponding azimuthal velocities (not shown), closely resemble the experimental measurements [5,7,10]. At the smallest ω there is no radial flow; when radial flow begins the z dependence is almost sinusoidal,

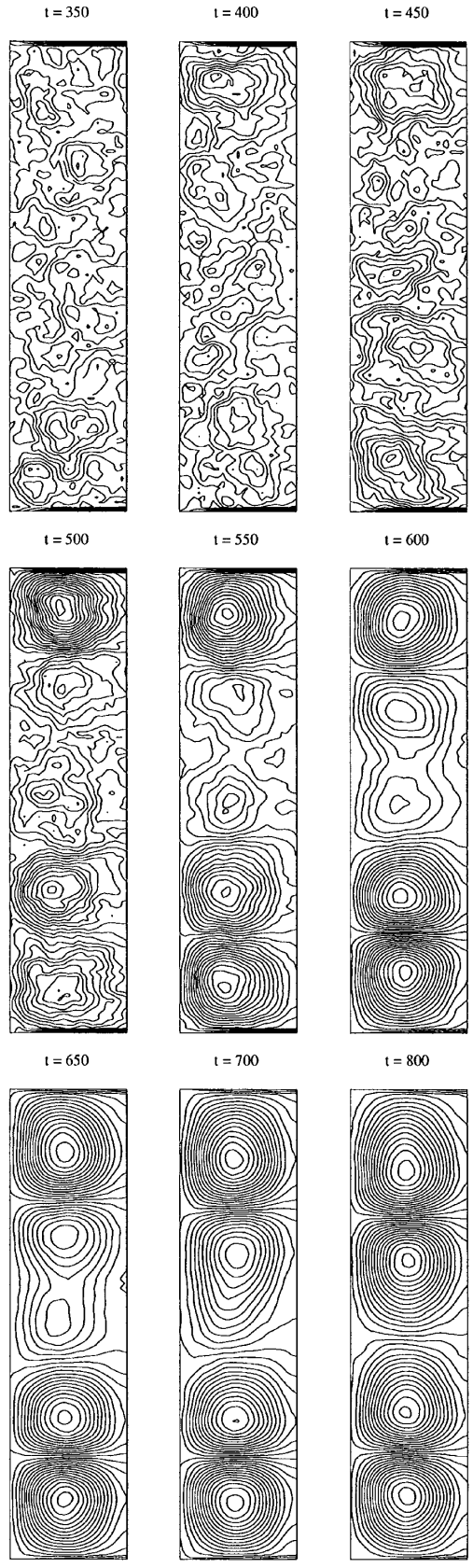

FIG. 1. Sequence of snapshots for $\omega = 0.1$ in which streamlines (azimuthally averaged) are used to show various stages of vortex development.

but deviations appear as ω increases, with the radial outflow becoming significantly faster than the inflow.

The form of $v_r(z)$ calls for Fourier analysis similar to that used in treating the experimental data, leading to the expansion in Eq. (1). The smooth curves included in Fig. 2 show the results of this calculation; here the fundamental ($n = 1$) mode and the first two harmonics are included, with wave number $q = 3.17/d$. Clearly, the principal features of the data are represented reasonably accurately by just three Fourier terms; adding a further harmonic has no noticeable effect on the fit. Typical error bars are shown; these reflect the fluctuations in the measurements that occur between samples.

Stability analysis [4] predicts that $q = 3.14/d$; the slightly larger q value needed here—the change produces a 1% shift in the positive peak positions, leading to a marginally improved fit for larger ω—is readily attributed to finite-size effects such as relatively thick radial boundary layers. The value of z_0 (used to accommodate slight deviations from axial symmetry) is adjusted for the best fit; its value lies in the range -1.8–$+0.8$ (for different ω), a less than 2% shift along the axis. It should be remembered that unlike the four vortices obtained here, experimentally $L \gg d$ and there are therefore many more vortices, so that Fourier analysis can exclude the end vortices that have been distorted by additional shear effects.

Theory [11] predicts that the Fourier coefficients $A_n(\epsilon)$ should have the form shown in Eq. (2). Experiments agree with this prediction, and the ability to fit the MD results to theory would provide convincing evidence that the MD approach captures the hydrodynamics in a quantitatively correct manner. The problem is that an "effective" Taylor number cannot be evaluated directly because it is a function of the viscosity, which in turn depends on the density, temperature, and shear rate, all of which vary substantially across the system. The results of the fit to the theoretical prediction are independent of ν, however;

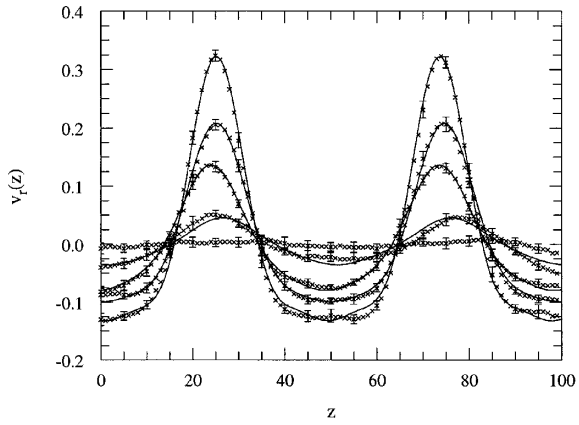

FIG. 2. Axial (z) variation of the mean radial velocity $v_r(z)$ with fits based on the first three terms of the Fourier expansion; the peaks become larger and the harmonics more pronounced as ω increases ($\omega = 0.055$, 0.06, 0.07, 0.08, 0.1).

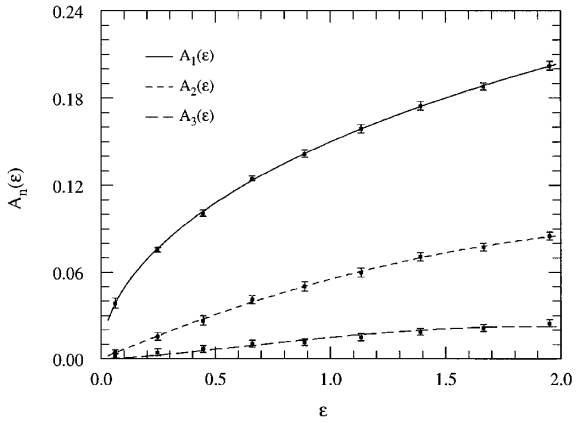

FIG. 3. The data points show the first three Fourier amplitudes of the mean radial velocity plotted as functions of $\epsilon = (T - T_c)/T_c$; the curves are based on fits to the theory that include only linear ϵ corrections.

we therefore simply assume that $\nu = 1$, a value typical of equilibrium simulations under the kinds of conditions prevailing here [18], and use this to compute R and T. Given this assumption, the values of R covered by the present simulations range from 75 to 125 (T range: 4500–12 500). The predicted critical value is $R_c = 76.6$ (corresponding to $T_c = 4690$) [4].

The value of T_c, and the coefficients of the $A_n(\epsilon)$ expansions in Eq. (2) to linear order in ϵ, can be obtained using least-squares fits to the Fourier results (refined estimates of T_c are also obtained in a similar manner from experimental data). First, independent estimates of T_c are extracted from the fits to A_1 and A_2; the values obtained are 4244 and 4223. These differ by less than 1%, so using their mean (which happens to correspond to a value of R_c only 5% below the theoretical value), and repeating the fits to obtain the expansion coefficients, yields $a_1 = 0.1554$ and $a_{11} = -0.0355$ for the fundamental, $a_2 = 0.0676$ and $a_{21} = -0.183$ for the first harmonic, $a_3 = 0.0196$ and $a_{31} = -0.283$ for the second. The ϵ dependence of the first three Fourier amplitudes is shown in Fig. 3. These fits are of similar quality to those obtained experimentally. (The error estimates shown are obtained by repeating the analysis for each of the 20 sets of measurements.) Since the linear ϵ corrections already provide an essentially perfect fit over the range $0 < \epsilon < 2$ there is no need to include the quadratic terms.

In conclusion, the results presented in this Letter show that molecular dynamics simulation is capable of capturing the details of the Taylor flow instability in a quantitatively correct manner. The simulations not only establish that continuum hydrodynamics remains valid at the extremely small length and time scales addressed by MD, but imply that MD is capable of becoming a useful tool for investigating complex flows. Indeed, the route to understanding the microscopic mechanisms underlying transitions between spatially distinct flow states is likely to require detailed MD analysis of suitably defined correlation functions in the transition region. Further study of the Taylor and other three-dimensional flow problems is currently in progress

Partial support for this work was provided by a grant from the Ministry of Science. The calculations were carried out on the IBM/SP2 computer at the Inter-University Computation Center.

[1] G. I. Taylor, Philos. Trans. R. Soc. London A **223**, 289 (1923).
[2] P. G. Drazin and W. H. Reid, *Hydrodynamic Stability* (Cambridge University Press, Cambridge, 1981).
[3] S. Chandrasekhar, *Hydrodynamic and Hydromagnetic Stability* (Oxford University Press, Oxford, 1961).
[4] R. C. Di Prima and H. L. Swinney, *Hydrodynamic Instabilities and the Transition to Turbulence*, edited by H. L. Swinney and J. P. Gollub (Springer, Berlin, 1981).
[5] R. J. Donnelly and K. W. Schwarz, Proc. R. Soc. London A **283**, 531 (1965).
[6] H. A. Snyder and R. B. Lambert, J. Fluid Mech. **26**, 545 (1966).
[7] J. P. Gollub and M. H. Freilich, Phys. Fluids **19**, 618 (1976).
[8] T. Berland, T. Jossang, and J. Feder, Phys. Scr. **34**, 427 (1986).
[9] R. M. Heinrichs *et al.*, Phys. Fluids **31**, 250 (1988).
[10] S. T. Wereley and R. M. Lueptow, Exp. Fluids **18**, 1 (1994).
[11] A. Davey, J. Fluid Mech. **14**, 336 (1962).
[12] P. S. Marcus, J. Fluid Mech. **146**, 65 (1984); M. Lücke, M. Mihelcic, and K. Wingerath, Phys. Rev. A **31**, 396 (1985).
[13] D. C. Rapaport and E. Clementi, Phys. Rev. Lett. **57**, 695 (1986); D. C. Rapaport, Phys. Rev. A **36**, 3288 (1987).
[14] M. Mareschal and E. Kestemont, J. Stat. Phys. **48**, 1187 (1987); D. C. Rapaport, Phys. Rev. Lett. **60**, 2480 (1988); M. Mareschal *et al.*, Phys. Rev. Lett. **61**, 2550 (1988); A. Puhl, M. M. Mansour, and M. Mareschal, Phys. Rev. A **40**, 1999 (1989); D. C. Rapaport, Phys. Rev. A **46**, 1971 (1992); **46**, R6150 (1992).
[15] D. C. Rapaport, *The Art of Molecular Dynamics Simulation* (Cambridge University Press, Cambridge, 1995).
[16] C. D. Andereck, S. S. Liu, and H. L. Swinney, J. Fluid Mech. **164**, 155 (1986).
[17] J. A. Cole, J. Fluid Mech. **75**, 1 (1976).
[18] D. M. Heyes, Comput. Phys. Rep. **8**, 71 (1988).